Available online at www.sciencedirect.com
SCIENCE DIRECT®
Journal of Nuclear Materials 337–339 (2005) 281–285
journal of nuclear materials
www.elsevier.com/locate/jnucmat

Plasma profiles and flows in the high-field side scrape-off layer in Alcator C-Mod

N. Smick [a,*], B. LaBombard [a], C.S. Pitcher [b]

[a] MIT Plasma Science and Fusion Center, NW17-170, 175 Albany St., Cambridge, MA 02139, USA
[b] 132 Bowood Ave., Toronto, Canada M4N1Y5

Abstract

A novel, magnetically-driven swing probe was recently installed near the midplane on the high-field side SOL in Alcator C-Mod. The probe collects plasma from co- and counter-current directions during its respective 0–90° and 90–180° of motion, thus providing profiles of density, electron temperature and plasma flow parallel to magnetic field lines (Mach number, $M_{\|}$) up to the separatrix. Results are reported from discharges with different magnetic topologies: lower single-null, upper single-null, and double-null. In single-null, a strong parallel flow ($|M_{\|}| \sim 1$) is detected, which is always directed from the low- to high-field SOL. In double-null discharges, e-folding lengths in the high-field SOL are a factor of ~4 shorter than the low-field SOL. Thus, plasma appears to 'fill-in' the high-field SOL in single-null plasmas, not by cross-field transport but by parallel flow from the low-field SOL – a picture consistent with a very strong ballooning-like component to the cross-field transport.
© 2004 Elsevier B.V. All rights reserved.

PACS: 52.55.Fa; 52.70.−m
Keywords: Alcator C-Mod; Cross-field transport; Edge plasma; Plasma flow; Probes

1. Introduction

The high-field side scrape-off layer (HFS-SOL) is perhaps one of the more poorly diagnosed regions of the edge plasma. The lack of diagnostic ports and the restricted space in high-field, high-performance tokamaks normally prohibits scanning Langmuir probes from operating in this region. Nevertheless, a host of interesting and potentially important phenomena are known to exist in this zone, including MARFES [1], strong plasma flows [2], and a sensitivity of the plasma profiles to magnetic topology (single versus double-null) [3].

With the goal of providing detailed, high spatial resolution plasma profile measurements near the midplane in the HFS-SOL, a novel, magnetically-driven fast-scanning swing-probe was installed in Alcator C-Mod. The actuation of the probe is based on an imbedded magnetic coil, with a construction similar to that used for the actuation of the divertor bypass 'flaps' on Alcator C-Mod [4]. This probe has proven capable of inferring density, electron temperature and parallel Mach number profiles up to the separatrix and has revealed key information about particle flows, poloidal asymmetries in cross-field particle and heat transport and their connections to magnetic topology.

In this paper, we report on the design of the probe (Section 2), its operation (Section 3), and representative plasma profile and flow results from a series of

* Corresponding author.
E-mail address: nsmick@mit.edu (N. Smick).

0022-3115/$ - see front matter © 2004 Elsevier B.V. All rights reserved.
doi:10.1016/j.jnucmat.2004.09.035

discharges in which the magnetic topology was varied between lower single-null, upper single-null, and double-null (Section 4).

2. Inner scanning probe (ISP)

A cross-sectional view of Alcator C-Mod is shown in Fig. 1, indicating the locations of two scanning probes: an 'outer scanning probe' positioned 10 cm above the midplane in the low-field side of the SOL (LFS-SOL) (described in Ref. [5]) and an 'inner scanning probe' (ISP) positioned 5 cm below the midplane on the HFS limiter. (Note: Ref. [6] erroneously indicates the ISP as being 5.8 cm *above* the midplane.) The internal construction and swing-motion of the ISP is illustrated in Fig. 1. The ISP consists of single 1.6 mm diameter electrode, flush with the tip of a carbon fiber composite arm (7.6 mm diameter) that protrudes from a rectangular carbon fiber composite body. The probe body pivots about a vertical axis in response to current in an embedded coil that interacts with the ambient magnetic field. A torsion spring mounted on the vertical shaft holds the probe against the wall when it is not being activated. When at its rest position (0°), the entire probe is 'hidden' behind the tiles so that no field lines connect the probe directly to the plasma. At 90°, the probe arm reaches ~12 mm into the plasma and at 180° it is again hidden. With careful positioning of the magnetic separatrix at the midplane, complete profiles from the wall to the separatrix are obtained. The design of the ISP allows the probe to first 'look' in one direction along the field lines,

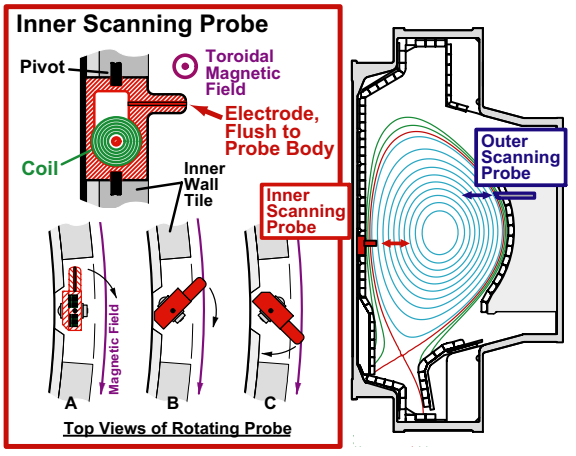

Fig. 1. Scanning Langmuir–Mach probes are used to infer simultaneously plasma profiles and parallel flows in the SOL on the low-field (outer scanning probe) and high-field (inner scanning probe) sides. The inner scanning probe is magnetically actuated with a swing motion, sampling plasma 'upstream' and 'downstream' along magnetic field lines.

then the other. The probe body is electrically isolated from the wall via ceramic insulators at the pivot axes.

The outer scanning probe employs four electrodes embedded in a floating molybdenum body, viewing both directions along field lines. This probe provides plasma profile and flow information in the LFS-SOL up to the separatrix, employing a pneumatically driven linear motion.

3. ISP operation

Fig. 2 shows a simple model for the coil drive circuit and some typical waveforms obtained during a 180° probe swing. Current flowing in the coil produces a magnetic moment, M, resulting in a torque that attempts to align the coil with the ambient toroidal magnetic field,

$$T_{\text{coil}} = MB\cos\theta. \tag{1}$$

Before a scan, a negative voltage is applied to hold the probe firmly against the wall and to allow a computation of the circuit resistance, R. When the voltage is switched positive, the probe arm begins rotating towards 90°. As the magnetic moment of the coil becomes aligned with the ambient field, the torque decreases. Therefore, only the probe's inertia can carry it past the 90° point. At this time, the voltage is programmed to reverse, reversing the direction of the magnetic dipole moment; the resultant torque continues to drive the probe towards 180°.

In order to infer the probe's position as a function of time, we use the back-EMF induced in the embedded coil,

$$V = IR + \underbrace{AB\cos\theta\frac{\mathrm{d}\theta}{\mathrm{d}t}}_{\text{Back-EMF}}. \tag{2}$$

Here, V is the applied voltage and IR is the resistive component of the voltage, computed from the measured current and circuit resistance. This relationship can be integrated to produce

$$\theta(t) = \arcsin\left(\frac{1}{AB}\int_{t_0}^{t}(V - IR)\,\mathrm{d}\tau\right). \tag{3}$$

Note that this procedure is valid only if B remains constant over the period of the integration, which is generally true for the discharges studied here. A is the effective area of the coil which is determined by requiring the maximum argument of arcsine to be unity.

An ambiguity arises from Eq. (3) as to whether the probe has passed beyond 90° or not. To address this issue, a series of trials were performed, varying the programmed duration of the positive voltage waveform and monitoring the probe motion with a camera. We identified a unique signature in the current trace that determines whether the probe passed 90° and learned the

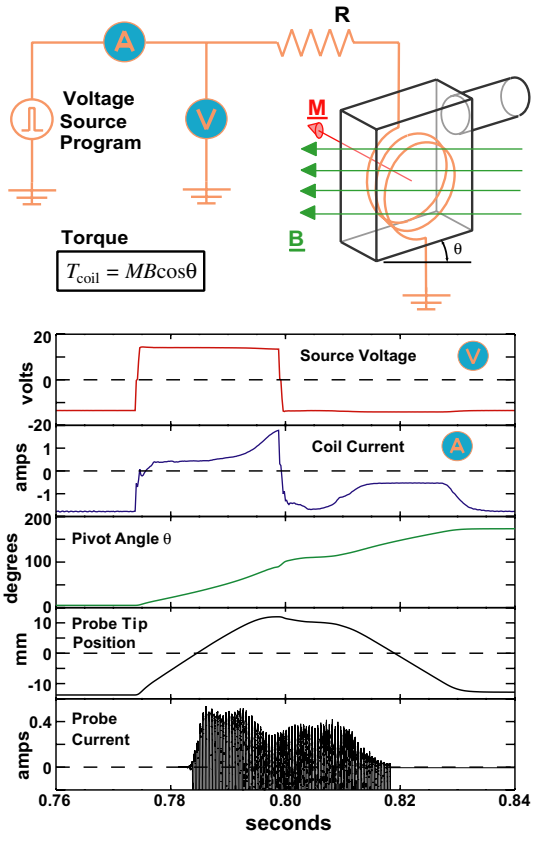

Fig. 2. Current flowing in the embedded coil of the Inner Scanning Probe interacts with the ambient magnetic field and applies a torque to the probe body. With an appropriately timed voltage source waveform, the probe body can be made to swing through 180° of arc, sampling plasma 12 mm beyond the edge of the inner wall tiles. Plasma density, electron temperature and floating potential are inferred over the electrode's trajectory by fitting to I–V characteristics at intervals of 0.25 ms. The resultant ion collection portion of the I–V sweep (positive current) is shown in the last panel.

appropriate positive voltage waveform durations for typical values of ambient magnetic field (~23 ms in Fig. 2).

The plasma parameters inferred by the ISP are density, floating potential, electron-temperature and flow velocity (along field lines). The first three are derived from fitting positive and negative-going I–V characteristics, generated by applying a 2 kHz triangular waveform of amplitude 200 V between the probe electrode and body. A typical current waveform showing positive (ion collection) portions of the I–V sweeps is shown in Fig. 2. Approximately 200 measurements are generated this way during a 50 ms one-way scan. The resulting spatial distance between measurement points is ~0.2 mm. The data is sampled at a rate of 1 MHz. Ion saturation current fluctuations in the frequency range of 5–500 kHz are monitored during time intervals when the probe is biased into saturation. Successive measurements of ion saturation current (I_{sat}) looking up and down the field lines are combined to determine the parallel Mach number of the plasma velocity using the Hutchinson formula,

$$M_{\parallel} = 0.43 \ln\left(\frac{I_{\mathrm{Sat,Up}}}{I_{\mathrm{Sat,Down}}}\right). \quad (4)$$

When the probe is near 90°, interpretation of the I–V characteristic becomes uncertain because the projected area of the electrode along the field lines approaches zero [7]. Consequently, we discard data taken between 80° and 100°. An appropriate correction for the projected area of the electrode along the field line is applied when calculating the absolute value of ion saturation current density (J_{sat}) at other angles. Irregularities in the carbon fiber composite arm and misalignment of the tungsten electrode can introduce asymmetries in the electrode's projected area near angles of 80° or 100°. Therefore, one must allow for the possibility of an offset to the inferred Mach flow measurements, particularly near the separatrix. However, such an offset would be constant and independent of plasma conditions or magnetic x-point topology.

4. Plasma flows and profiles

Utilizing the new inner scanning probe, a series of experiments were performed to compare plasma profiles and flows in the LFS- and HFS-SOLs and map out their sensitivities to magnetic x-point topologies (upper, lower, double-null). Representative results from a set of matched discharges are shown in Figs. 3 and 4. These were ohmic L-mode plasmas ($I_p = 0.78$ MA, $B_T = 5.4$ T, $\bar{n}_e = 1.4 \times 10^{20}$ m^{-3}) with B_T and I_p aligned and $B \times \nabla B$ pointing down. (Comprehensive information on plasma flow observations in these and other discharge conditions is available in a separate publication [6].) The color-coded profiles (red – HFS-SOL, blue – LFS-SOL) are smooth spline curves, fitted to data points recorded over the probes' trajectories. The data are plotted versus the magnetic flux surface coordinate, ρ, which is the distance into the SOL mapped along field lines to the LFS midplane. Shaded areas are locations that map to limiter surfaces. Triangles indicate data recorded by electrodes 'facing up' or 'facing down' along magnetic field lines. Density (n), electron temperature (T_e) and fluctuation data (the RMS ion saturation current fluctuation about the mean divided by the mean) are derived separately for the 'facing up' and 'facing down' electrodes; no correction is applied to account for background plasma flow. However, an algebraic average of the 'facing up' and 'facing down' densities is a good first approximation to the ambient density, independent of

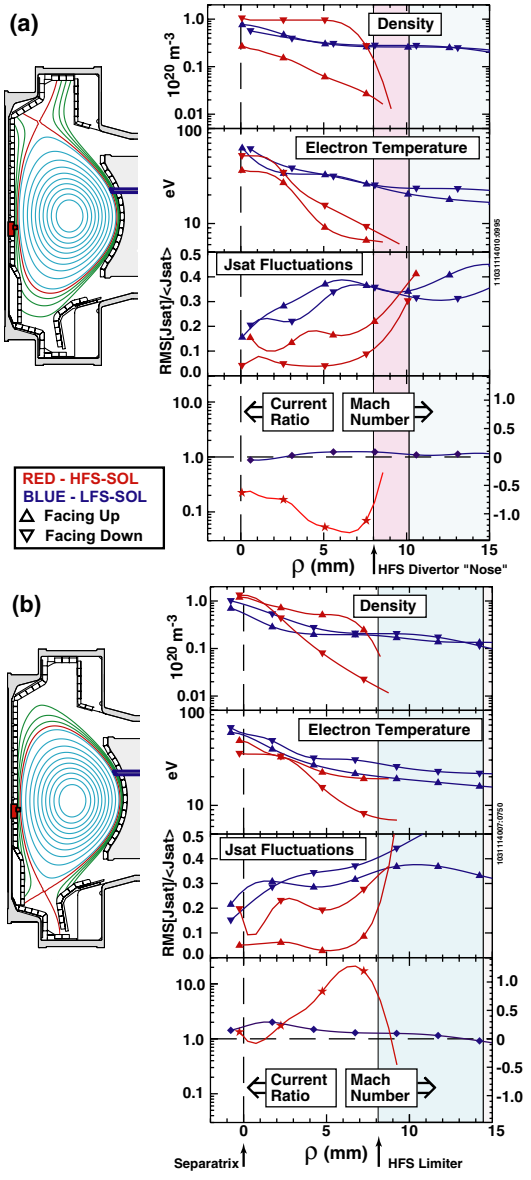

Fig. 3. Upper single-null (a) and lower single-null magnetic equilibria (b) and the corresponding plasma profiles on the high-field side (red) and low-field side (blue) scrape-off layers. Triangles indicate data taken from electrodes that are facing 'up' (to the top of the vessel) or 'down' along magnetic field lines. The parallel Mach number of the flow is estimated from the ratio of ion saturation currents when looking 'up' versus 'down'. Positive Mach number is defined as having a toroidal projection in the co-current direction. In the upper single-null case (a), the field lines between high- and low-field SOLs are broken by the inner divertor 'nose'. The resulting private-flux region on the high-field side is indicated by the purple shaded region.

plasma flow velocity. The ratios of ion saturation current densities and the parallel Mach numbers computed

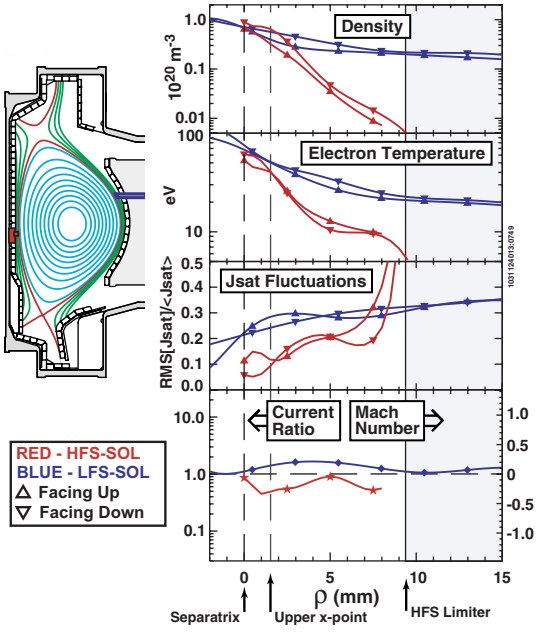

Fig. 4. Scrape-off layer profiles in a near double-null equilibrium and with plasma conditions matched to those of the discharges in Fig. 3.

from Eq. (4) are also shown. Positive Mach number corresponds to the toroidal component of flow being in the co-current (I_p) direction.

A number of important results can be discerned from the data in Figs. 3 and 4. In single-null topologies (Fig. 3), the electron pressure, nT_e, is found to approximately map from LFS- to HFS-SOL along field lines. However, T_e is systematically lower and n higher in the HFS-SOL. In addition, T_e in the HFS-SOL has a directional dependence: it is lowest looking in the direction of the HFS divertor, independent of x-point location. These observations point to a ballooning-like heat transport asymmetry: heat entering into the LFS-SOL conducts down T_e gradients along field lines toward the HFS divertor.

The most dramatic features in Fig. 3 are the near-sonic plasma flows seen on the HFS-SOL. These flows flip from co- to counter-current direction when changing from lower to upper null, apparently to maintain a flow of particles from the LFS- to HFS-SOL regions. Thus, the origin of this flow appears to be connected to the ballooning-like transport asymmetry. Flows on the LFS-SOL are generally weaker. We typically find these to be co-current directed, modulated by magnetic topology (increasingly co-current in the sequence upper, double, lower-null) and reduced in magnitude at high densities. They appear to be dominated by plasma rotation and/or Pfirsch–Schlüter flows [6,8]; only a weak flow component associated with ballooning-like transport asymmetries appears at this LFS midplane location.

In all topologies (Figs. 3 and 4), the normalized ion saturation current fluctuation levels are significantly lower on the HFS-SOL than the LFS-SOL (factor of ~5 in single-null topologies when a flow-corrected ambient ion saturation current is used in the normalization). These data are consistent with optical measurements of plasma fluctuations on the HFS- and LFS-SOLs [9]. These observations again imply a ballooning-like transport phenomenon where much of the turbulent cross-field transport is occurring across the LFS separatrix. The difference between upstream and downstream normalized fluctuation levels in the HFS-SOL is primarily due to the lower time-averaged J_{sat} observed when looking downstream (a consequence of the strong flows in this region).

A comparison of n and T_e profiles in near double-null discharges (Fig. 4) reveals a dramatic reduction in the plasma pressure on the HFS-SOL: pressure e-folding lengths are a factor of ~4 shorter in double versus single-null topologies. This is perhaps the most compelling evidence of a strong ballooning-like character to cross-field particle transport. The parallel flow on the HFS-SOL is seen to be relatively stagnant in double null, as expected if the near-sonic flows of Fig. 3 are primarily driven by HFS/LFS pressure asymmetries along magnetic field lines.

5. Summary

Near-sonic parallel flows ($|M| \sim 1$) directed from LFS- to HFS-SOL in single-null topologies are detected by a novel scanning probe installed on the HFS limiter in Alcator C-Mod. Low fluctuation levels are measured at this location, independent of topology, while sharp pressure gradients and reduced flow are recorded in double-null plasmas. Thus, a strong ballooning-like asymmetry in cross-field heat and particle transport is evident. Plasma appears to 'fill-in' the HFS-SOL in single-null plasmas, not by cross-field transport but by parallel flow from the LFS-SOL.

Acknowledgments

These results were made possible by the efforts of the entire Alcator team and support from the US. D.O.E. Coop. Agreement DE-FC02-99ER54512.

References

[1] B. Lipschultz et al., Nucl. Fus. 24 (1984) 977.
[2] D. Jablonski et al., J. Nucl. Mater. 241–243 (1997) 782.
[3] C.J. Boswell, J.L. Terry, B. LaBombard, B. Lipschultz, C.S. Pitcher, Plasma Phys. Control. Fus. 46 (2004) 1247.
[4] C.S. Pitcher et al., Rev. Sci. Instrum. 72 (2001) 103.
[5] B. LaBombard, Phys. Plasmas 9 (2002) 1300.
[6] B. LaBombard et al., Nucl. Fus. 44 (2004) 1047.
[7] G.F. Matthews et al., Plasma Phys. Control. Fus. 32 (1990) 1301.
[8] B. LaBombard, S. Gangadhara, B. Lipschultz, C.S. Pitcher, J. Nucl. Mater. 313–316 (2003) 995.
[9] J. Terry, S. Zweben, O. Grulke, M. Greenwald, B. LaBombard, 2004, these Proceedings. doi:10.1016/j.jnucmat.2004.10.092.